CALT-767-P3-32

COMPUTER ENHANCEMENT OF WEAK-BEAM IMAGES*

by

H.M. Horgen and R. E. Villagrana
W. M. Keck Laboratory of Engineering Materials
California Institute of Technology
Pasadena, California 91109

and

D.M. Maher
Bell Laboratories
Murray Hill
New Jersey 07974

*This investigation was sponsored by the U.S. Atomic Energy Commission

COMPUTER ENHANCEMENT OF WEAK-BEAM IMAGES

In order to perform quantitative image-contrast analysis of low-contrast electron micrographs one must first increase the signal to noise ratio. As an example, consider the weak-beam method[1,2] of imaging defects by transmission electron microscopy. In this technique an increase in the resolution of closely spaced dislocations is obtained through a narrowing of the individual dislocation image widths. However, this reduction in image width is accompanied by a corresponding decrease in the signal to noise ratio, which in many instances renders quantitative image-contrast analysis impractical. In this note we present an example of the computer image enhancement of a weak-beam micrograph.

The computer image processing was carried out as follows:

(i) Three weak-beam images of the same area were digitized at a high sampling density (25μ) (Fig. 1).

(ii) The gray levels of these images were then spread linearly over the full dynamic range (Figs. 1 and 2).

(iii) Random points of bad data, which gave rise to the appearance of "snow", were removed by a local averaging process.

(iv) Statistical random noise, due to the film grain and quantum electron noise, was attenuated by a factor of $\sqrt{3}$ by superimposing three pictures (Fig. 3). The translational and rotational registration was determined by cross-correlation over the area of the rectangle shown in Fig. 1.

(v) A one-dimensional low-pass box filter was applied along the length of the dissociated dipole (Fig. 4).

At various stages in the computer processing, optical density curves were taken across the dissociated dipole (Figs. 5, 6, 7). Finally, figures 6 and 7 were smoothed using a Fourier series expansion (Figs. 8, 9). In figures 8 and 9 the individual peaks of the dissociated dipole are now revealed.

References

1. A. Howie and Z.A. Basinski, Phil. Mag. 17, 1039 (1968).
2. D.J.H. Cockayne, I.L.F. Ray and M.J. Whelan, Phil. Mag. 20, 1265 (1969).

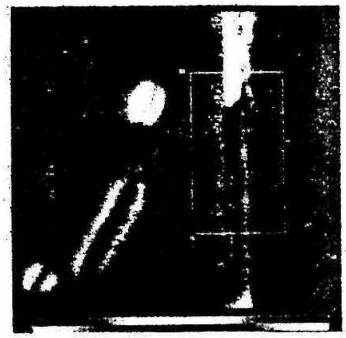

Fig. 1. Digitally displayed weak-beam image of dislocations in Ge. Frame shows the area (682 x 682 Å) used for subsequent processing.

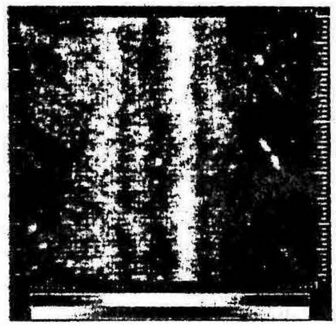

Fig. 2. Dissociated dipole image after positioning and linear contrast stretch (196 x 196 Å).

Fig. 5. Intensity profile of Fig. 2 taken 35 Å from the top of the picture. (All subsequent profiles are taken at the same position.)

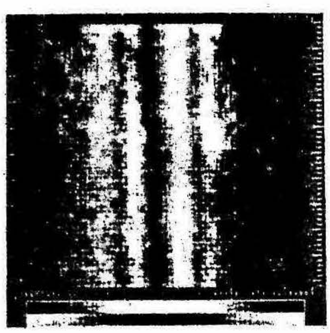

Fig. 3. Averaged picture resulting from the superposition of three micrographs.

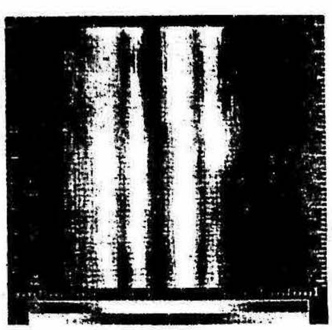

Fig. 4. Low-pass box filtered version of Fig. 3.

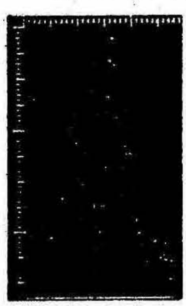

Fig. 6. Intensity profile of Fig. 3.

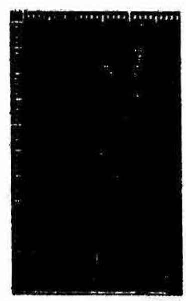

Fig. 7. Intensity profile of Fig. 4.

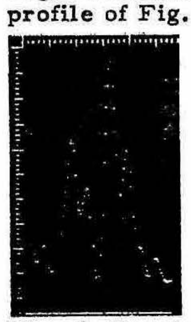

Fig. 8. Fourier smoothing of Fig. 6.

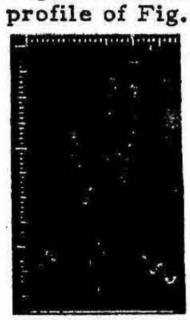

Fig. 9. Fourier smoothing of Fig. 7.